Mobile Channel Sounder Validations Carried Out at the ITS Table Mountain Field Site

Robert Johnk[1], Erik Hill[1], Chriss Hammerschmidt[1], Anna Paulson[1], Ronald Carey[1], Savio Tran[1], Mike Chang[1]

[1]Institute for Telecommunication Sciences (ITS), Boulder, Colorado USA

Contact: rjohnk@ntia.doc.gov

Abstract— **We present path gain results at 3,500 MHz from a mobile channel measurement campaign that was carried out at the ITS Table Mountain Field Site. The purpose of this effort was to validate measurements obtained from a prototype sliding correlator channel sounder that is currently under development at ITS. The validation framework we developed consists of two parts: 1) a CW channel sounder to provide a highly accurate reference, and 2) a series of static paths and a mobile route over which to compare path gain results from the two systems. We obtained excellent agreement in measured path gains between the sliding correlator and the CW systems.**

Keywords—Antenna, Correlation CW, Down Convertor, GPS, Irregular Terrain Mode (ITM), Mixer, Measurement Comparison, Path Gain, Longley-Rice, Mobile, Propagation, Rubidium Frequency Reference, Sliding Correlator, Spectrum Analyzer, Time Series, Time Variations, Vector Signal Analyzer

I. INTRODUCTION

Engineers from NTIA's Institute for Telecommunication Sciences (ITS) have been developing a new and innovative sliding correlator (SC) channel sounder since 2016 under the sponsorship of NTIA's Office of Spectrum Management (OSM) [1]. This SC system development has been carried out under the guidance of Dr. Christopher R. Anderson of the U.S. Naval Academy [1],[2]. The SC will provide ITS with a flexible, high-resolution tool to perform propagation measurements in a wide variety of outdoor radio channel environments. Since development began, this system has been deployed in several measurement campaigns in both rural and urban environments. ITS engineers plan to use the radio propagation data obtained from this system to develop improved models that OSM, in turn, can use to provide accurate and better-informed spectrum policy decisions. At this time, OSM is primarily interested in path gain at 3,500 MHz between a fixed transmitter and a mobile receiver for a variety of both rural and urban radio propagation environments.

A critical issue that the ITS engineering team is addressing is the accuracy of the sliding correlator for path gain measurements. The approach that we are taking has several elements: 1) Direct comparisons of the sliding correlator channel sounder with an ITS-developed precision continuous-wave (CW) measurement system in mobile channel drive testing [3]. 2) A sequence of drive tests that start with open and uncluttered regions (rural) and progress to more complex cluttered environments (urban). 3) A harmonized thru-calibration procedure for both the SC and the CW channel sounder that ensures good measurement precision.

In summary, the approach we are using is to start with open environments and progress to more heavily cluttered urban areas. Throughout this process, we will provide direct comparisons of measured path gains from the sliding correlator to those obtained with the precision CW system.

II. OVERVIEW OF THE TABLE MOUNTAIN TESTS

Our first measurement campaign was carried out at the ITS Table Mountain (TM) Field Site and Radio Quiet Zone, which is located 20 km north of Boulder, Colorado. The TM field site is uncluttered, and radio propagation is dominated by terrain. We set up our CS transmitters at a fixed location on top of the TM plateau and deployed our CS receiving systems in a van. We then performed a series of drive tests with the van driving over prescribed routes. The drive routes provide both line of sight (LOS) and non-line-of-sight (NLOS) conditions. The NLOS conditions were caused by terrain blockage. The level of clutter (e.g. vegetation, buildings) is minimal throughout the selected drive routes at TM.

We installed both the SC receiver and the CW receiver in the van. We configured the transmitter to transmit at a frequency of 3,500 MHz for both SC and CW path gain measurements. For the SC measurements, a BPSK modulation was applied to the transmitter at center frequency of 3,500 MHz using a pseudorandom-noise (PN) sequence. Due to electromagnetic interference (EMI) concerns [4], only one channel sounder was active for a given drive test. We also performed a series of static propagation measurements with the van parked at different locations. We selected both LOS and NLOS paths for the static measurements. This combination of mobile and static path gain measurements provides a rich set of data for both comparisons and system validations.

In order to obtain high level of accuracy, we implemented a thru-calibration procedure for each channel sounder. Before a mobile or static test, we connect the transmitter and receiver feed cables through a high-power attenuator with accurately known characteristics. This procedure provides an accurate reference signal that is compared directly with the over-the-air drive test signal levels. By maintaining the same transmit and receive system configurations in the over-the-air tests and the thru calibration, we can now directly measure path gain.

III. SLIDING CORRELATOR CHANNEL SOUNDER

The sliding correlator system consists of a transmitter and a receiver. Fig. 1 shows the block diagram of the transmitter.
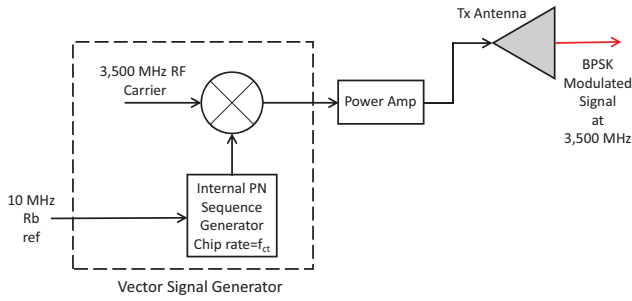
Fig. 1. The sliding correlator transmitter.

The transmitter consists of a commercial off-the-shelf (COTS) vector signal generator (VSG) that is programmed to operate at a carrier frequency of 3,500 MHz. The transmitted signal is BPSK modulated using a pseudo-noise (PN) binary sequence. For the TM tests, we used a maximal length sequence of length 511 and a chip rate of f_{ct} =5 Mcps. At this chip rate, the PN sequence has a period of 102.2 µs, and the transmitted bandwidth is approximately 20 MHz after filtering [1]. The modulated sequence signal is then boosted by a power amplifier to a level in the range 1-10 W at the transmitting antenna input for the drive tests.

Fig. 2 shows block diagram of the SC receiver. The signal from the antenna is routed to a preselector that amplifies and filters the signal, to both improve sensitivity and filter out unwanted interfering signals.

The preselector output is fed into a dual down convertor box in Figs. 2 and 3. Inside this box, there are two mixers and a combination of low-pass and band pass filters located at the mixer ports. The first mixer local oscillator port is fed with a BPSK-modulated PN sequence with a carrier frequency of 3,660 MHz. This PN sequence is an exact replica of the transmitted PN sequence, but at a chip rate that is now 250 cps slower than the transmitted sequence with a chip rate of 4.99975 Mcps. This difference in chip rates creates a sliding effect between the transmit and receive PN sequences that greatly reduces the sampling rate requirements at the receiver, along with the signal bandwidth. The first mixer output is a down-converted replica of the original signal with a center frequency of 160 MHz and a bandwidth of 20 MHz (after filtering).
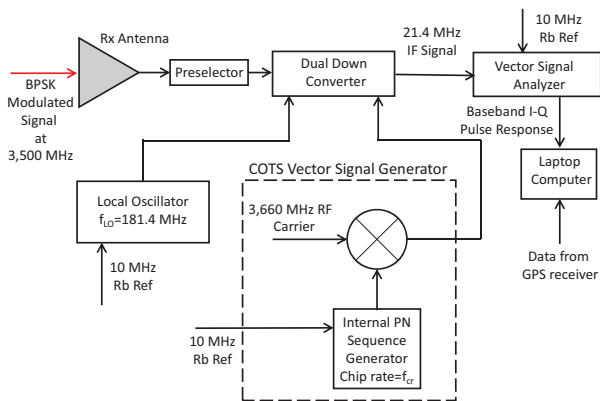
The output of the first mixer is fed into a second mixer stage that has a 181.4 MHz CW local oscillator. The resulting output is down converted to a center frequency of 21.4 MHz, which, in turn, is filtered using a phase-linear, band pass filter. The resulting spectrum is now only 1 kHz wide. The net effect of these stages of mixing is to compress the spectrum bandwidth from 20 MHz to 1 kHz—a factor of 20,000! This bandwidth compression also has the benefit of reducing the required sampling rate by the same factor, which greatly reduces required data acquisition rates and the amount of data that needs to be processed.

The final stage of processing occurs when the filtered 21.4 MHz IF signal is fed into the input port of a vector signal analyzer (VSA). The VSA digitizes, filters, and down-converts the signal to a baseband in-phase and quadrature (I-Q) format that is post-processed using a computer. Fig. 3 shows the ITS sliding correlator system undergoing a benchtop conducted performance evaluation at the ITS laboratories. Precise control of the center frequencies of the transmitter signal generator and the receiver generators is provided by 10 MHz rubidium frequency references that are synchronized prior to testing.

The combination of the dual down conversion hardware and the VSA filter settings directly generates the cross-correlation function of the transmitted and received PN sequences. This is all done by the system hardware and no-post processing is needed to generate the correlation. However, a time dilation occurs due to the different chip rates and the sliding effect between the transmitter and the receiver. The amount of time dilation is determined from the slide factor which is given by

$$\gamma = \frac{f_{ct}}{(f_{ct} - f_{cr})} \quad , \qquad (1)$$

where f_{ct} and f_{cr} are the transmitter and receiver chip rates, respectively. For the TM tests, we used a slide factor of 20,000, with a resulting correlation period of 2.04 s. The resulting I-Q output sample rate is only 1.25 kHz—a huge reduction over the required Nyquist sampling rate of 20 Ms/s that would be needed for a full-bandwidth PN channel sounder [5]. Another major benefit of using a SC channel sounder is not having to post-process large amounts of digitized data as is required with a full bandwidth PN channel sounder. Molisch [5] provides an excellent explanation of the sliding effect and how the reduction of the required sampling rate is realized.
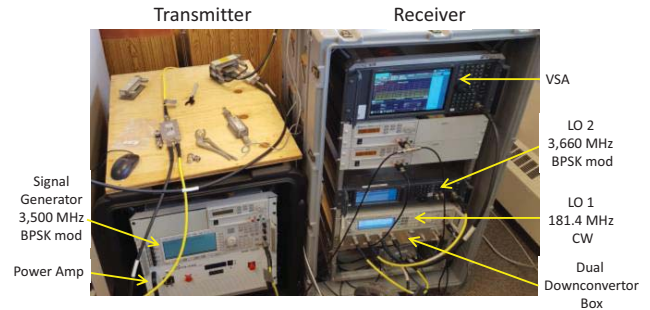

Fig. 2. The sliding correlator receiver.

Fig. 3. The sliding correlator set up for conducted accuracy tests.
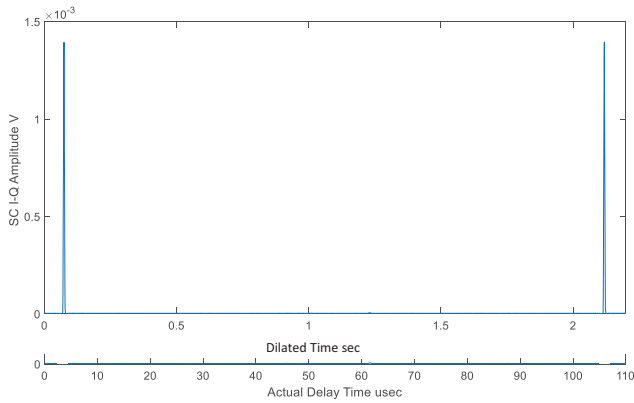
464

Fig. 4. Sliding output voltage amplitude recorded by the VSA. The actual propagation delay is obtained by dividing the dilated time by the slide factor of 20,000.
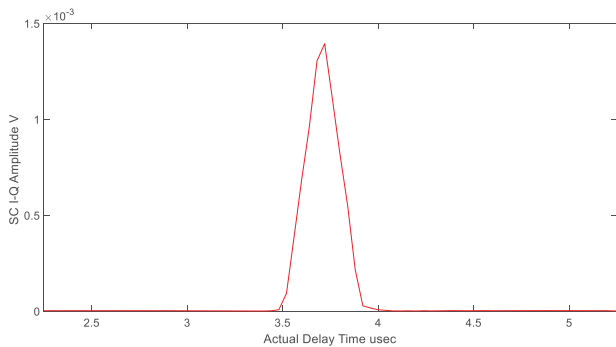

Fig. 5. Triangular pulse sliding correlator output obtained from a conducted bench test at the output of the sliding correlator.

Fig. 4 and Fig. 5 show SC outputs obtained from a benchtop conducted test. In this case, the SC I-Q envelope is a sequence of triangular-shaped pulses. The dilated time is what we measure at the SC output with the VSA. In order to compute actual propagation delay, we divide the dilated time by the slide factor given in (1). The output I-Q envelope is plotted for both dilated and actual time scales in Fig. 4.

IV. ITS CW CHANNEL SOUNDER

Fig.6 and Fig. 7 show functional diagrams of the transmitter and receiver sections of the CW channel sounder. The details of this channel sounder are provided in [3]. The transmitter consists of a COTS signal generator that feeds a 3500 MHz CW signal into a power amplifier that boosts the signal level at the antenna input.

The received signal is split equally by a power divider and routed to a spectrum analyzer and a VSA. The spectrum analyzer serves as a real-time signal monitor and it provides geolocation information from its built-in GPS receiver. The other half of the received signal is directed to a VSA that converts the received signal to baseband I-Q that is post-processed to obtain desired propagation parameters. The sampling rate for the VSA was set at 3,840 ks/s with a corresponding bandwidth of 3 kHz for the TM tests. We used a one-second moving average window to remove fast-fading effects and to provide an estimate of path gain. The signal processing details are described in [3].
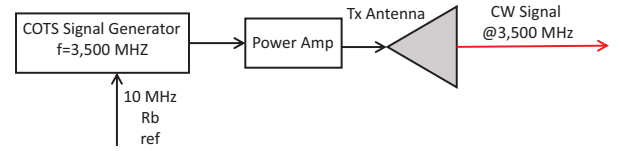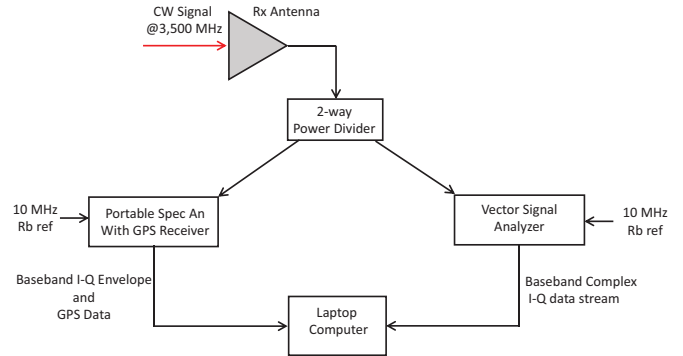

Fig.6. The CW channel sounder transmitter.

Fig. 7. The CW channel sounder receiver.

V. HARMONIZED CALIBRATION OF THE CHANNEL SOUNDERS

We developed a thru-calibration procedure to achieve accuracy, time-efficiency, and simplicity in our measurement procedures. We also wanted to calibrate both the CW and SC systems using the same procedure to obtain high accuracy in our channel sounder comparisons.

Fig. 8 depicts the calibration procedure that we used for the channel sounder comparisons. The insertion gain between the antennas is given by:

$$IG = P_{ra}/P_{ta} \quad , \tag{2}$$

where P_{ta} is the amount of forward power delivered into the transmit antenna port and P_{ra} is the power delivered from the receiver antenna feed connector to the receiver feed line. In order to measure IG using (2), we need to carefully calibrate the transmitter and receiver antenna feed networks using a vector network analyzer and measure signal power at the transmitting and receiving antenna ports directly. This approach requires care and can be labor intensive, depending on the number of components that are evaluated.

An alternative approach is to perform a two-step relative measurement of signal power at the receiver input using the configurations shown in Fig. 8. We now measure the power at the receiver input port only. The first configuration is a mobile drive test and we measure the received power, which we denote as P_{rd}. In the second configuration, we disconnect the feedlines from the transmitting and receiving antennas and connect them directly through a high-power attenuator with a known attenuation level A. We then measure the receiver power P_{ratt}. The insertion gain is now given by

$$IG\ (dB) = 10\ log_{10}\left(\frac{P_{rd}}{P_{ratt}}\right) + A(dB)\ , \tag{3}$$
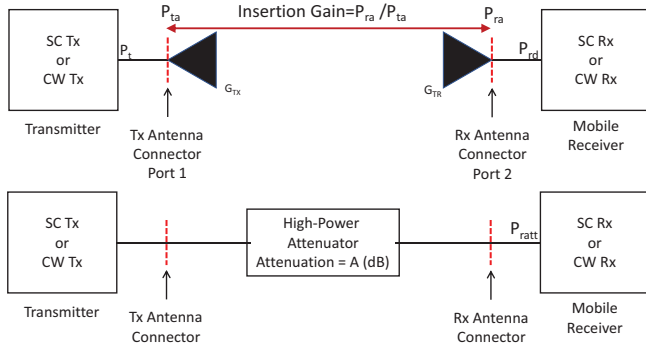
465

Fig. 8. The thru-calibration used for the channel sounder comparisons.

From (3), we see that this is relative measurement with both power measurements being made at the receiver input. We now add antenna gain corrections to obtain the path gain

$$PG\ (dB) = IG\ (dB) - G_{tx}\ (dB) - G_{rx}\ (dB)\ , \qquad (4)$$

where G_{tx} is the gain of the transmitting antenna and G_{rx} is the gain of the receiving antenna. Equations (3) and (4) are applicable to both the CW and SC channel sounders, but the methods we use to compute the receiver power are somewhat different.

For the SC channel sounder, we compute the time average of the squared amplitude of the I-Q time series. In the TM mobile testing, we compute the time-average power over one period of the SC output I-Q time series.

For the static testing that is described later in section VII, we computed the time average over multiple periods. For the CW channel sounder, we also post process the output from the VSA. In this case, the output is not periodic, and we apply a one-second moving average window to the squared magnitude of the I-Q time series to compute the receiver power [3].

VI. TABLE MOUNTAIN TESTING

We performed testing of the SC and CW channel sounders at the Table Mountain Test Site at 3,500 MHz. We placed the channel sounder transmitters in an all-weather cabinet that is mounted on a cell on wheels (COW). The COW has an extendable mast and we mounted a 9 dBi omni antenna transmitting on the top of the mast at a height of 6.1 m. We located the transmitter on the top of Table Mountain as is shown in Fig. 9. The SC and CW channel sounder receivers were mounted in the van as shown in Fig. 10.

The van has an extendable mast on which we mounted a 2 dBi omni antenna. The van was deployed in two different modes: 1) We drove the van over a prescribed route on the Table Mountain road and captured mobile data while the van was being driven at a nominal speed of 20 mph (9.8 m/s), 2) We parked the van at different locations and captured static data for a period of five minutes (300 s). For both the static and the mobile measurements, we carried out one set of measurements with the CW system and then repeated the drive tests with the SC channel sounder. The primary advantage of this sequential

testing is that we only had one system on the air at a time and this avoids serious EMI effects due to system nonlinearities [4].

At the beginning of each testing sequence, we connected both the transmitting and receiving antenna feed lines to an 82 dB high-power attenuator. This is a robust, full-system calibration that includes all the system elements, including the transmitter power amplifier. Fig. 11 shows a thru calibration being carried out for the SC channel sounder at the transmitter site.

Fig. 9. The COW deployment on top of Table Mountain.

Fig. 10. The mobile receiving van on the main north-south road at the Table Mountain Field Site.

Fig. 11. Channel sounder thru calibration at the transmitter site.

466

VII. MOBILE DRIVE TEST RESULTS

The mobile drive test route that we used for the channel sounder comparisons is shown in Fig. 12. It consists of six primary navigation waypoints. The test begins at waypoint 1, near the west entrance to the TM test site on Plateau Rd. The white circled area around waypoint 1 denotes NLOS conditions between the transmitter and the receiver due to terrain blockage by the mountain. The van drives east from the gate and climbs to the top of TM and LOS conditions occur once the top is reached. The route continues for 2 km past the main north-south road, and the van turns around in the parking lot of a building at waypoint 2. The route then continues to the intersection of Plateau Rd. at waypoint 3 and proceeds north 1.6 km to waypoint 4. There is a small hill near waypoint 4 and the route drops into NLOS conditions due to a small ridge. The van turns around and heads south to Plateau Rd. at waypoint 5 and then west to the gate at waypoint 6 and back into NLOS conditions.

Fig. 13 shows the measured path gain time series for the SC and CW channel sounders the mobile drive test route of Fig. 12. We also performed a series of point-to-point predictions using an ITS-developed MATLAB® implementation of the Longley-Rice Irregular-Terrain model (ITM) to provide a theoretical comparison [6]. The agreement obtained in measured path gains is excellent in the LOS portions of the drive tests. Significant variations are seen near waypoint 1, and we attribute this to time variations in the channel and the fact that the measurements were performed at different times. The ITM results agree quite well in the LOS portions of the drive test. More significant discrepancies between ITM and the measurements are seen in the NLOS portions of the route. ITM is known to underpredict path gain close to terrain obstructions, and this is the case here. We also see discrepancies between measurement and theory near waypoint 2, which are caused by the blockage effects of a nearby building. ITM does not account for clutter effects.

VIII. STATIC TESTS

We also performed two series of independent static tests for the setup shown in Fig. 14. We parked the receiving van at the five locations shown in Fig. 14 (note: the numbers of the static locations are not the same as the previous mobile waypoints). Positions 1-3 are LOS, and positions 4 and 5 are NLOS due to terrain obstructions. We parked the van at each location and captured data for five minutes. We did this for the SC system first and then switched over to the CW channel sounder and repeated the measurement sequence.

We observed time variations in the radio channel during the data acquisitions. For the LOS paths, we observed variations in path gain that were in the range of roughly 0.3 dB over a 300 s interval. These variations occurred over time intervals of 5-10 s. The characteristics of the time variability changed dramatically at the NLOS measurement points. The time variations for NLOS static measurements are considerably more complex. In this case, we saw variations in path gain of approximately 5 dB over time scales of 3-5 s and variations of 10 dB for time scales in the range of 50-150 s. These variations are due to the radio channel. More study is needed to understand the cause of these time variations.
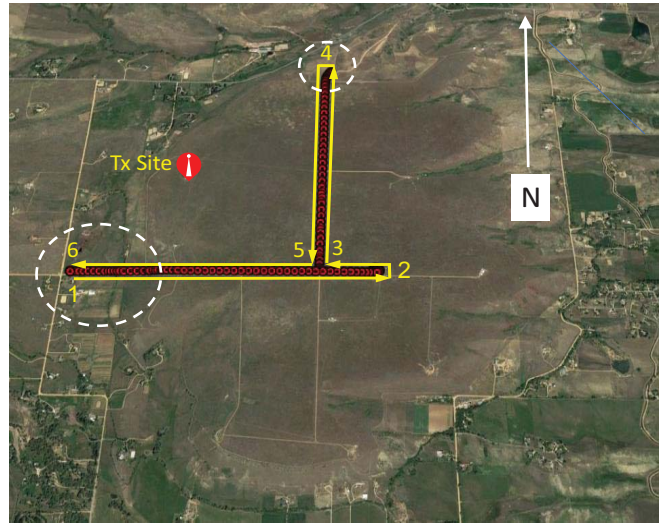

Fig. 12. Mobile drive test route for the channel sounder comparisons at the TM test site. The dashed circles denote areas where the receiver is in a NLOS region.
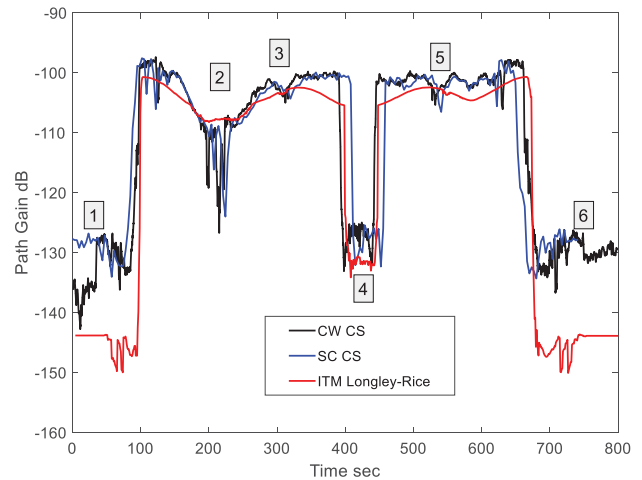

Fig. 13. 3,500 MHz path gain time series for the SC and CW channel sounders along computed ITM results. The plot is annotated with the numbered waypoints.
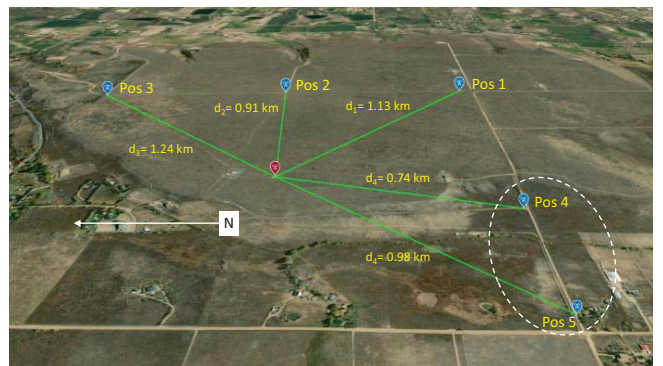

Fig. 14. Static test locations for the TM channel sounder comparisons.

467

Table 1 provides a summary of the SC and CW channel sounder basic path gain data that we obtained from the static tests. The results are obtained from a 300 s average of the data obtained at each static location. Excellent agreement between the channel sounder measurements is obtained at positions 1–3 and 5. A significant discrepancy between the channel sounder measurements is seen at position 5. We attribute this to a couple of things. First, position 5 has the highest level of terrain blockage and the lowest level of path gain of all the locations. Second, we also saw time variations of approximately 10 dB in the received signal over the 300 s data acquisition period. We see very good agreement between ITM and channel sounder results for the LOS positions. ITM underpredicts path gain for the NLOS positions 4 and 5, and we see significant deviations.

TABLE I.   PATH GAIN RESULTS FOR STATIC TESTS.

Position	Tx-Rx Distance (km)	Sliding Correlator Channel Sounder Path Gain (dB)	CW Channel Sounder Path Gain (dB)	ITM Longley-Rice Path Gain (dB)
1 (LOS)	1.13	-105.3	-105.1	-104.4
2 (LOS)	0.91	-103.5	-102.8	-102.3
3 (LOS)	1.24	-104.0	-103.4	-105.2
4 (NLOS)	0.74	-134.0	-141.7	-147.6
5 (NLOS)	0.98	-127.3	-127.2	-144.2

IX. CONCLUSIONS

We performed a series of comparisons between a new sliding correlator channel sounder that is under development at ITS and a precision CW channel sounder at 3,500 MHz. We designed a series of drive tests at the ITS TM Field Site to compare the two channel sounders. The TM Field Site was ideal for testing because it is accessible and uncluttered. Radio propagation is dominated by terrain effects.

We developed a harmonized thru-calibration procedure for both channel sounder systems that improves both measurement efficiency and accuracy. We then performed a series of outdoor measurements at the ITS Table Mountain Test site. We conducted both mobile drive tests around a prescribed route and a series of static tests with a mobile receiving van parked at fixed locations.

We performed the testing sequentially, with only one channel sounder being active at a time to avoid EMI effects. The agreement between the two systems was generally quite good. The highest discrepancies were seen in NLOS zones, which is due primarily to changes in channel characteristics between tests. The comparison tests clearly demonstrate that the sliding correlator can accurately measure path gain

The plan moving forward is to perform further comparisons of the SC and CW channel sounders in more complex environments that have clutter due to structures and vegetation. We also plan to enhance the accuracy of our measurement systems by accounting for component mismatch errors in our calibrations [7].

REFERENCES

[1] Erik Hill and Christopher R. Anderson, "A high performance pseudorandom noise sliding correlator channel sounder," NTIA Technical Report in preparation.

[2] Christopher R. Anderson, Design and implementation of an ultrawideband millimeter-wavelength vector sliding correlator channel sounder and in-building multipath measurements at 2.5 & 60 GHz, M.S. Thesis, Virginia Polytecnic University, 2002.

[3] Robert Johnk, Chriss Hammerschmidt, Irena Stange, "A high-perfromance CW channel sounder," IEEE Int. Symp. EMC and Signal/Power Integrity , August 7-11, 2017 pp. 698-703.

[4] Robert T. Johnk, "Propagation measurement pathologies," 2018 International Symposium on Advanced Radio Technologies (ISART), July 26, 2018.

[5] Andreas Molish, Wireless communications, John Wiley & Sons Ltd., New York, New York, 2011.

[6] George A. Hufford, Anita G. Longley, William A. Kissick, A guide to the use of the ITS irregular terrain model in the area prediction mode, NTIA Technical Report 82-100, April 1, 1982.

[7] Glenn F. Engen, Microwave circuit theory and foundations of microwave metrology, Peter Perigrinus, United Kingdom, 1992.